Hindawi Publishing Corporation
Journal of Nanomaterials
Volume 2012, Article ID 475430, 6 pages
doi:10.1155/2012/475430

Research Article

Photoelectrochemical Properties of Fe_2O_3 Supported on TiO_2-Based Thin Films Converted from Self-Assembled Hydrogen Titanate Nanotube Powders

Kyung-Jong Noh,[1] Hyo-Jin Oh,[1] Bo-Ra Kim,[1] Sang-Chul Jung,[2] Wooseung Kang,[3] and Sun-Jae Kim[1]

[1] *Institute/Faculty of Nanotechnology and Advanced Materials Engineering, Sejong University, Seoul 143-747, Republic of Korea*
[2] *Department of Environmental Engineering, Sunchon National University, Sunchon 540-742, Republic of Korea*
[3] *Department of Metallurgical & Materials Engineering, Inha Technical College, Incheon 402-752, Republic of Korea*

Correspondence should be addressed to Wooseung Kang, wkang651@inhatc.ac.kr and Sun-Jae Kim, sjkim1@sejong.ac.kr

Received 6 April 2012; Revised 16 June 2012; Accepted 16 June 2012

Academic Editor: Jiaguo Yu

A photoanode was fabricated using hematite (α-Fe_2O_3) nanoparticles which had been held in a thin film of hydrogen titanate nanotubes (H-TiNT), synthesized by repetitive self-assembling method on FTO (fluorine-doped tin oxide) glass, which were incorporated via dipping process in aqueous $Fe(NO_3)_3$ solution. Current voltage (I-V) electrochemical properties of the photoanode heat-treated at 500°C for 10 min in air were evaluated under ultraviolet-visible light irradiation. Microstructure and crystallinity changes were also investigated. The prepared Fe_2O_3/H-TiNT/FTO composite thin film exhibited about threefold as much photocurrent as the Fe_2O_3/FTO film. The improvement in photocurrent was considered to be caused by reduced recombination of electrons and holes, with an appropriate amount of Fe_2O_3 spherical nanoparticles supported on the H-TiNT/FTO film. Nanosized spherical Fe_2O_3 particles with about 65 wt% on the H-TiNT/FTO film showed best performance in our study.

1. Introduction

Hydrogen production through photoelectrochemical (PEC) water splitting process has been paid much attention as a promising solution to the global energy problem [1–4]. Transition metal oxide semiconductors have been considered candidate materials as a photoelectrode for this process. Among them, one of the most extensively explored materials is Fe_2O_3-based materials with optical energy bandgap of ~ 2.2 eV [5–7]. However, some major issues have been raised in the fabrication of a Fe_2O_3 photoanode as well as electrocatalyst, such as low electrical conductivity of the material itself and necessity of less than 5 nm particle synthesis, to avoid electron-hole recombination related to the extremely short diffusion distance of holes, among others [8, 9]. Along with the transition metal oxide semiconductors, TiO_2 with optical energy bandgap of 3.0~3.2 eV has also been much investigated as an electrode material due to its favorable characteristics, such as photoelectrochemical stability, nontoxicity, and low cost for fabrication [10–12]. In our present study, we focused on the fabrication and optimization of nanosized Fe_2O_3 supported on TiO_2-based nanotube materials for PEC cell performance for the water splitting process. The materials are expected to exhibit the advantages of the porous TiO_2-based nanotube thin film support, as they are fully utilized to enhance the photoelectrochemical performance of supported Fe_2O_3 nanoparticles.

To overcome the aforementioned limitations in the PEC application, in this paper, porous TiO_2 film converted by heat treatment from the H-TiNT (hydrogen-titanate nanotube) film fabricated by repetitive self-assembling method on the FTO substrates was utilized to support Fe_2O_3 nanoparticles. The materials were characterized, and their I-V PEC

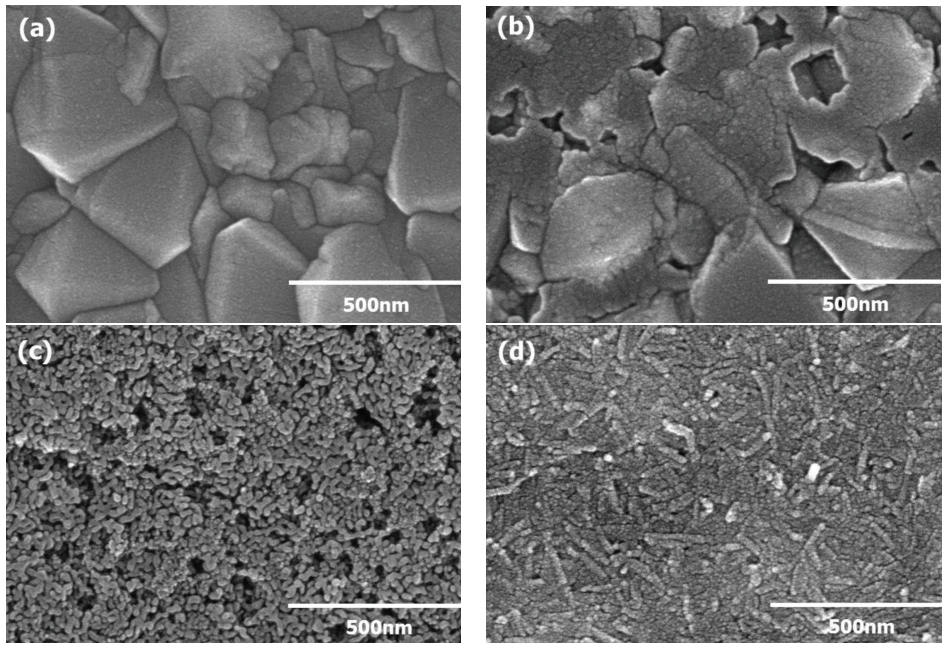

Figure 1: SEM surface images of Fe oxide and TiNT films coated on the FTO substrate; (a) FTO film, (b) Fe oxide (Fe2O3 = 27.16 wt%)/FTO film, (c) Fe oxide (Fe2O3 = 100 wt%)/FTO film, and (d) H-TiNT/FTO film, which were heat-treated at 500∘C for 10 min in air.

performance under ultraviolet-visible (UV-Vis) light irradiation for the water splitting process was carefully investigated to optimize the Fe_2O_3 particles on the support.

2. Experimental Procedure

Repetitive self-assembling of oppositely charged ions in an aqueous solution was applied to directly coat the H-TiNT powder, which was obtained from a hydrothermal technique detailed in our previous reports, on a transparent conducting substrate of FTO glass [13–17]. FTO glass (Asahi Glass Co.) used as a transparent conductive substrate was surface-treated for 20 min in 0.2 M polyethyleneimine (PEI, Aldrich) aqueous solution containing positively charged ions. All the aqueous solutions were prepared using distilled water of 1.8 MΩ. The surface-pretreated FTO glass was immersed for 20 min in an aqueous 10 g/L H-TiNT solution dispersed together with 0.2 M tetrabutylammonium hydroxide (TBAOH, Aldrich) to produce negatively charged ions. Using the same method, an H-TiNT-treated film was subsequently immersed in 0.2 M polydiallyldimethylammonium chloride (PDDA, Aldrich) aqueous solution containing positively charged ions. Repetition of these processes yielded an H-TiNT film coated on the FTO glass with approximately 700∼1000 nm thickness as previously reported in our research [15–17]. The obtained H-TiNT/FTO glass was dried under UV-Vis light irradiation (Hg-Xe 200 W lamp, Super-cure, SAN-EI Electric) to remove water and all the surfactants, such as PEI, TBAOH, and PDDA using photocatalytic removal reaction occurred by H-TiNT particles with the optical energy bandgap of 3.5 eV [16], without any sintering. Then, for the Fe_2O_3 nanoparticle coating process, the dried H-TiNT/FTO substrates were dipped in an aqueous 1.0 M $Fe(NO_3)_3$ solution for 6∼24 hrs. It was also done by multiple dipping of the samples in the solution along with the heat treatment after each dipping, at 500°C for 10 min in air atmosphere. In order to have thin thickness of the Fe_2O_3 film which has a bandgap of 2.2 eV, the optical energy bandgap of the Fe_2O_3/H-TiNT/FTO samples was controlled to be in the range of 3.24∼2.9 eV. The heat treatment was done inside a box furnace with the heating rate of 500°C/sec to produce the final photoanode thin film with α-Fe_2O_3 phase, where the rapid heating rate was accomplished by plunging the samples into the hot zone of the furnace maintained at 500°C.

The microstructures, crystallinities, optical energy band gap, and I-V electrochemical properties of the as-prepared heat-treated thin films were analyzed using scanning electron microscopy (SEM; S-4700, Hitachi), Raman spectroscopy (Renishaw, inVia Raman microscope), UV-Vis spectroscopy (S-3100, Sinco), and cyclic voltammetry (μAutolab type III, Micro Autolab), respectively. To measure the I-V electrochemical property, a calomel electrode and a Pt wire were used as the reference and counter electrodes, respectively, when the Fe_2O_3/H-TiNT composite film was used as the working electrode in an aqueous 1.0 M NaOH deaerated solution under irradiation of 130 mW/cm^2 UV-Vis spectrum (Hg-Xe 200 W lamp, Super-cure, SAN-EI Electric). The measured potentials versus calomel electrode were converted to the reversible hydrogen electrode (RHE) scale.

3. Results and Discussion

Figure 1 displays the SEM photos for the surface microstructures of the Fe oxide and the H-TiNT films coated as a photoanode material on the pure FTO substrate, which were all heat-treated at 500°C for 10 min in air. Figure 1(a) is the

surface of the heat-treated FTO substrate with 300~500 nm sized grains and a roughness of ±200 nm. Figures 1(b) and 1(c) are the images of Fe oxide films with 27.16 and 100 wt% of Fe_2O_3, respectively, coated on the surface of the FTO substrate after multiple dips in an aqueous 1 M $Fe(NO_3)_3$ solution, drying, and heat treatment. Here, the amounts of Fe_2O_3 were calculated by multiplying the measured concentration of combined elements of Sn and Fe by energy-dispersive spectroscopy, assuming a complete conversion of $Fe(NO_3)_3$ to Fe_2O_3. Figure 1(d) illustrates the H-TiNT film on the FTO substrate obtained by the repetitive self-assembling method as described in the experimental procedure. Figure 1(b) depicts the FTO substrate partially covered with less than 10 nm wide Fe_2O_3 particles. Figures 1(c) and 1(d) present the FTO substrate fully covered with 10~30 nm sized Fe_2O_3 particles and H-TiNT nanoparticles, respectively. It can be seen in Figure 1(d) that the H-TiNT nanoparticles consist of spherical and longitudinal particles transformed from ~10 nm wide and ~100 nm long tubular-shaped particles. It was confirmed by SEM and TEM techniques that the films in Figures 1(c) and 1(d) have less than 1 μm thick film coatings, especially Figure 1(d) was 700~1000 nm thick [15]. To confirm the phase or crystallinity of the specimens in Figures 1(a), 1(c), and 1(d), the Raman spectra are presented in Figure 2. The crystallographic characteristics of heat-treated FTO, Fe_2O_3, and H-TiNT films were also compared with those of the untreated FTO film (not shown). From the micrographs in Figure 1 and the corresponding Raman spectra in Figure 2, the microstructure of the heat-treated sample was found to consist of spherical α-Fe_2O_3, longitudinal titanate, and the spherical anatase TiO_2 phase, which was similarly observed and reported in our previous work [16].

The specimens in Figure 1 were initially applied to the photoanode for the water splitting process, where their *I-V* electrochemical characteristics were evaluated using a linear sweep voltammetry in the range of +0.7~+1.5 V versus the RHE under 130 mW/cm^2 UV-Vis light illumination (Figure 3). The current signals of all the specimens were detected with an onset voltage of around 0.9 V versus RHE. Both the heat-treated FTO and H-TiNT/FTO films yielded relatively very low currents up to the applied potential of 1.3 V versus the RHE, indicating that water splitting is electrochemically difficult at 1.23 V versus RHE. When the Fe_2O_3 film partially covered the FTO substrate (Fe_2O_3 = 27.16 wt%), its current significantly increased (1.39 mA/cm^2) at 1.23 V versus RHE, whereas the Fe_2O_3 film, which fully covered the surface of the FTO substrate, yielded a relatively low value, although higher than those of the heat-treated FTO and H-TiNT/FTO films. This variation indicates that not all the currents generated by the thick or full Fe_2O_3 film coating can be completely collected through the FTO conducting layer, compared with those generated by the thin or partial Fe_2O_3 film coating. As shown in Figures 1(b) and 1(c), it is thought that the collection of electrons in these specimens was not perfectly accomplished by the 5~30 nm Fe_2O_3 particles due to the typical recombination of electron hole [18, 19], although the amount of generated electrons on the thick or full Fe_2O_3 film coating on the FTO substrate

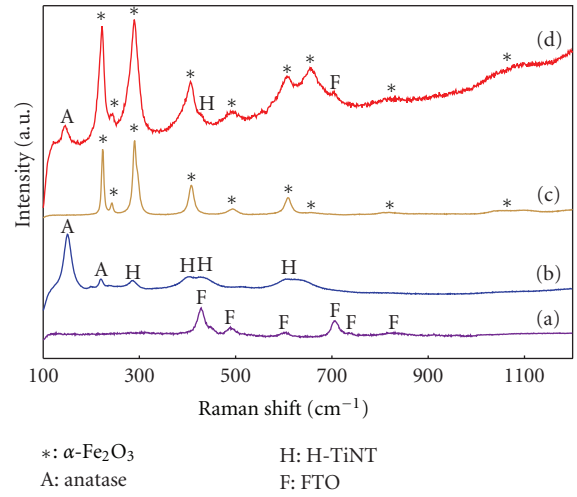

FIGURE 2: Raman spectra of (a) FTO, (c) Fe_2O_3/FTO, and (d) Fe_2O_3/H-TiNT/FTO film, which were heat-treated at 500°C for 10 min in air, comparing with that of (b) H-TiNT/FTO heat-treated at the same condition.

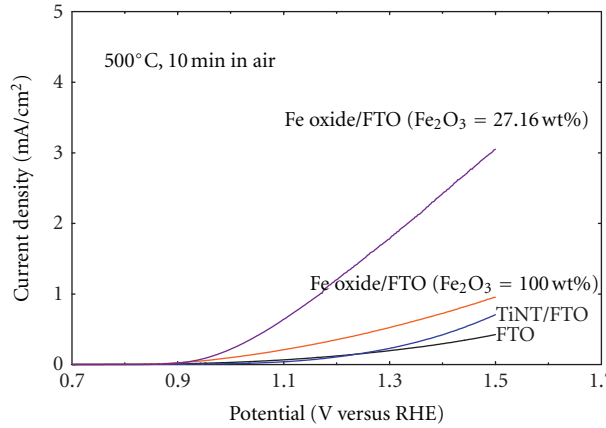

FIGURE 3: *I-V* characteristic curves for FTO film, and H-TiNT/FTO and Fe oxide (Fe_2O_3 with 27.16 and 100 wt%)/FTO films.

with UV-Vis light irradiation could become ample enough. Thus, it is obviously known that the amount or size of the Fe_2O_3 particles supported on the FTO substrate should be appropriately controlled to increase the current. However, because it was found that the current decreased abruptly with the Fe_2O_3 more than 27.16 wt% as in our preliminary experiments, our focus should be directed to the reduction of the Fe_2O_3 particle size or the insertion of a new easy path layer to the FTO substrate beneath the Fe_2O_3 film for energy band alignment. It would be more effective to protect the recombination of electrons and holes photogenerated in real system. Various amounts of Fe_2O_3 nanoparticles were supported on an H-TiNT/FTO composite film using the self-assembling or dipping procedure, as shown in Figure 4.

Figures 4 and 5 show the *I-V* electrochemical characteristics curves and the current at 1.23 V versus RHE, with varied Fe_2O_3 amounts supported on an H-TiNT/FTO composite film by controlling the dipping time or multiple

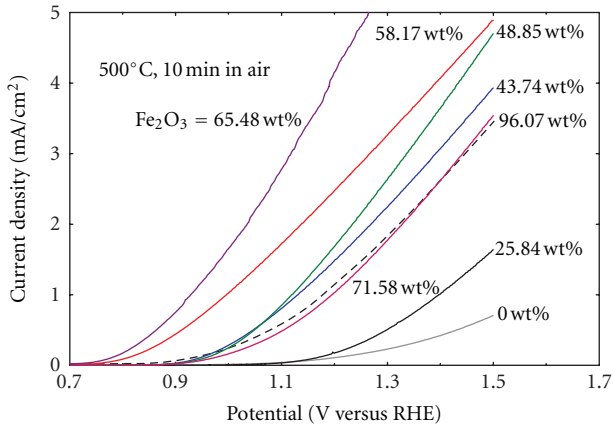

FIGURE 4: *I-V* characteristic curves for Fe_2O_3 films with various amounts of 0~100 wt% supported on H-TiNT/FTO film, followed by heat treatment at 500°C for 10 min in air. Here, 0 wt% means that there are no Fe_2O_3 particles on H-TiNT/FTO film and 100 wt% means Fe_2O_3 particles covered fully on the surface of the film.

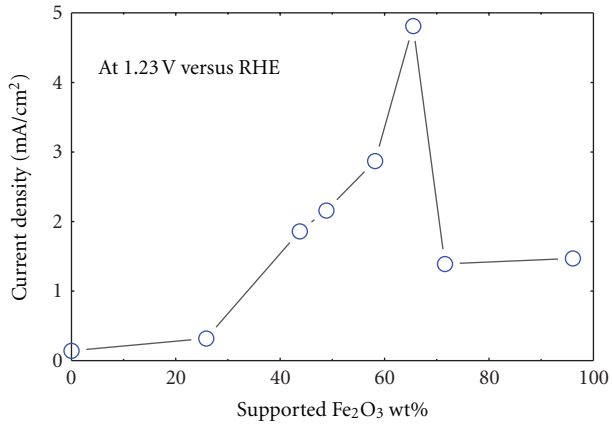

FIGURE 5: Current at 1.23 V versus RHE from *I-V* electrochemical characteristic curves of Figure 4.

dippings in an aqueous $Fe(NO_3)_3$ solution, respectively. This was followed by heat treatment at 500°C for 10 min in air to obtain the hematite-Fe_2O_3 phase. Here, the amount of Fe_2O_3 was also calculated by multiplying the measured concentration of combined elements of Ti and Fe by energy-dispersive spectroscopy, assuming a complete conversion of TiO_2 and Fe_2O_3 from H-TiNT and $Fe(NO_3)_3$. As the supported amount of Fe_2O_3 nanoparticles increases, the onset voltage decreases to approximately 0.7 V versus RHE, whereas their generated current significantly increases. The current density increase can be easily understood by the reasoning that more Fe_2O_3 involved due to the advantage of TiO_2 in the sample would enhance the visible light absorption. Performance improvements were similarly observed with the integrated materials, for the same purpose as ours, such as Fe-modified TiO_2 nanotubes [20] and CuS/ZnS porous nanosheets [21]. As shown in Figure 5, the current at 1.23 V versus RHE peaks at 4.81 mA/cm^2 with 65.48 wt% of the supported Fe_2O_3 nanoparticles on the H-TiNT/FTO film, which is about threefold as much current as the Fe_2O_3/FTO film. The generated current then decreases abruptly and would become saturated to approximately 1.4 mA/cm^2 due to formation of thick Fe_2O_3 film.

Figure 6 shows the representative SEM photos of the surface microstructures of the H-TiNT/FTO film supporting various amounts of Fe_2O_3 nanoparticles of Figure 4, which were obtained at 500°C for 10 min heat treatment. The Fe_2O_3 nanoparticles observed on the SEM surfaces with the amounts, when compared to Figure 6(d) which evidently covered the entire surface of the film, are different than the heat-treated H-TiNT/FTO (Figure 1(d)). At 96.07 wt% Fe_2O_3, the H-TiNT surface is almost perfectly covered by thick and more than 5 nm Fe_2O_3 particles similarly to those in Figure 1(c), although the surfaces fully covered with Fe_2O_3 nanoparticles had some pores. It was checked in preliminary work that the specimen of Figure 1(c) had about 2.9 eV of the optical energy bandgap, which means obtainment of thin Fe_2O_3 layer because bulky Fe_2O_3 material has about 2.2 eV. However, when covered with Fe_2O_3 nanoparticles, approximately more than 70 wt% of the specimens yielded relatively low current, still indicating the existence of a large recombination of electrons and holes photogenerated because their values are larger than those in the Fe_2O_3/FTO film. Consequently, it can be known that the maximum current can be obtained after heat treatment when supporting the appropriate amount of hematite-Fe_2O_3 nanoparticles around 65 wt% on the H-TiNT/FTO film. When the Fe_2O_3/FTO film is compared with the H-TiNT/FTO film, the H-TiNT coating cannot yield enough current. However, this coating can contribute greatly to the generation of an enhanced current as an easy path layer by reducing the recombination of electrons and photogenerated holes. Although Fe_2O_3 nanoparticles produce current, larger amounts or thick Fe_2O_3 nanoparticles result in the partial collection of generated current at the FTO electrode by increasing losses such as the recombination of electrons and holes and leakage current by high resistivity of Fe_2O_3 film. Thus, it can be said from our data that the insertion of an easy electron path layer beneath the Fe_2O_3 top layer is necessary to enhance the current for an efficient water splitting process. In the near future, our studies will be focused in detail on the importance and effect of the H-TiNT film to support Fe_2O_3 nanoparticles to increase the collected current at the FTO substrate. This can be conducted by the easy collection of photogenerated electrons from a Fe_2O_3 top layer, with controlled nanosizes of less than 10 nm, through detailed characterizations of H-TiNT and Fe_2O_3 materials.

4. Conclusions

To overcome the limitations of the Fe_2O_3 material for PEC application, H-TiNT film prepared by the repetitive self-assembling method on the FTO substrate was utilized to support Fe_2O_3 nanoparticles.

The $Fe(NO_3)_3$/H-TiNT composite films were heat-treated at 500°C for 10 min in air with very rapid heating rate of 500°C/sec. The materials were characterized, and their *I-V* electrochemical performance under UV-Vis light irradiation

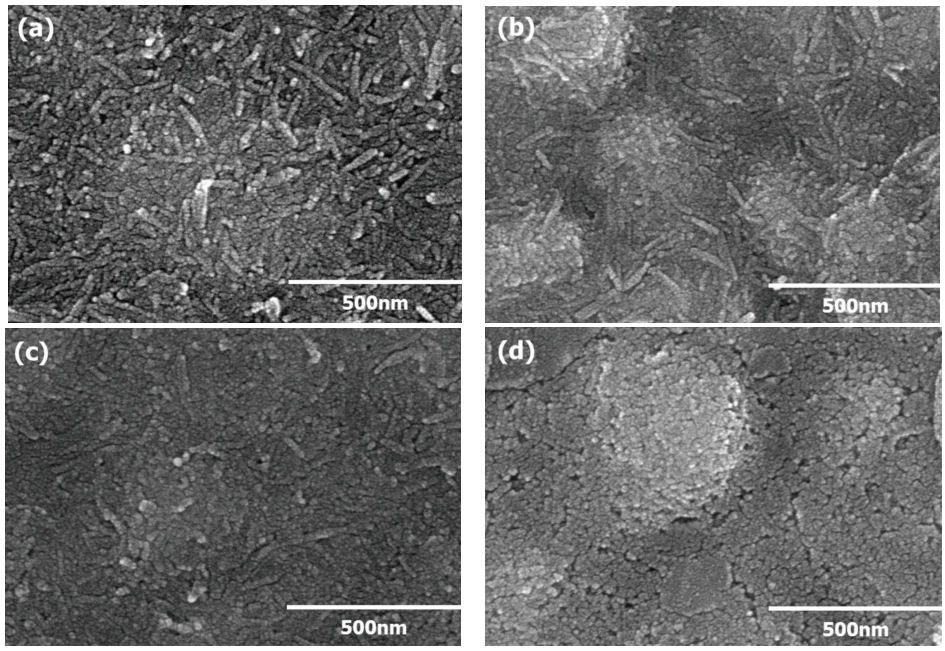

Figure 6: SEM surface images of Fe_2O_3 films with various amounts of (a) 25.84 wt%, (b) 65.48 wt%, (c) 71.58 wt%, and (d) 96.07 wt% supported on the H-TiNT/FTO film and finally heat-treated at 500°C for 10 min in air.

for the water splitting process was carefully investigated to determine the optimized Fe_2O_3 particle content. The heat-treated hematite-Fe_2O_3 phase film showed superior generation and collection of current with appropriate amounts of Fe_2O_3 on the H-TiNT film, with mixture of a longitudinal titanate phase and a spherical anatase TiO_2 phase. The onset voltage at 65.48 wt% supported Fe_2O_3 decreased to approximately 0.7 V versus RHE, and its current peaked at 4.81 mA/cm^2 at 1.23 V versus RHE. Although the Fe_2O_3 nanoparticles produced current, larger amounts or thick Fe_2O_3 nanoparticles resulted in a loss of generated current by increasing the recombination of electrons, holes, and leakage current by high resistivity of Fe_2O_3 film, and so forth. In conclusion, it can be suggested that the insertion of an easy electron path layer beneath the Fe_2O_3 top layer is necessary to enhance the current for an efficient water splitting process.

Acknowledgment

This paper was supported by the Basic Science Research Program through the National Research Foundation of Korea (NRF) funded by the Ministry of Education, Science and Technology (no. 2011–0016699).

References

[1] A. Fujishima and K. Honda, "Electrochemical photolysis of water at a semiconductor electrode," *Nature*, vol. 238, no. 5358, pp. 37–38, 1972.

[2] P. Kumar, P. Sharma, R. Shrivastav, S. Dass, and V. R. Satsangi, "Electrodeposited zirconium-doped α-Fe_2O_3 thin film for photoelectrochemical water splitting," *International Journal of Hydrogen Energy*, vol. 36, no. 4, pp. 2777–2784, 2011.

[3] P. R. Mishra, P. K. Shukla, and O. N. Srivastava, "Study of modular PEC solar cells for photoelectrochemical splitting of water employing nanostructured TiO_2 photoelectrodes," *International Journal of Hydrogen Energy*, vol. 32, no. 12, pp. 1680–1685, 2007.

[4] Y. Sun, C. J. Murphy, K. R. Reyes-Gil et al., "Photoelectrochemical and structural characterization of carbon-doped WO_3 films prepared via spray pyrolysis," *International Journal of Hydrogen Energy*, vol. 34, no. 20, pp. 8476–8484, 2009.

[5] E. Thimsen, F. Le Formal, M. Grätzel, and S. C. Warren, "Influence of plasmonic Au nanoparticles on the photoactivity of Fe_2O_3 electrodes for water splitting," *Nano Letters*, vol. 11, no. 1, pp. 35–43, 2011.

[6] S. Y. Sina, V. Bala, and W. K. Upul, "Microwave-assisted low temperature fabrication of nanostructured α-Fe_2O_3 electrodes for solar-driven hydrogen generation," *International Journal of Hydrogen Energy*, vol. 35, no. 19, pp. 10155–10165, 2010.

[7] T. Bak, J. Nowotny, M. Rekas, and C. C. Sorrell, "Photo-electrochemical hydrogen generation from water using solar energy. Materials-related aspects," *International Journal of Hydrogen Energy*, vol. 27, no. 10, pp. 991–1022, 2002.

[8] A. L. Stroyuk, I. V. Sobran, and S. Y. Kuchmiy, "Photoinitiation of acrylamide polymerization by Fe_2O_3 nanoparticles," *Journal of Photochemistry and Photobiology A*, vol. 192, no. 2-3, pp. 98–104, 2007.

[9] S. Kuang, L. Yang, S. Luo, and Q. Cai, "Fabrication, characterization and photoelectrochemical properties of Fe_2O_3 modified TiO_2 nanotube arrays," *Applied Surface Science*, vol. 255, no. 16, pp. 7385–7388, 2009.

[10] Y. Guo, X. Quan, N. Lu, H. M. Zhao, and S. Chen, "High photocatalytic capability of self-assembled nanoporous WO_3 with preferential orientation of (002) planes," *Environmental Science and Technology*, vol. 41, no. 12, pp. 4422–4427, 2007.

[11] Z. Zhang, M. F. Hossain, and T. Takahashi, "Self-assembled hematite (α-Fe_2O_3) nanotube arrays for photoelectrocatalytic

degradation of azo dye under simulated solar light irradiation," *Applied Catalysis B*, vol. 95, no. 3-4, pp. 423–429, 2010.

[12] J. Matos, J. Laine, and J. M. Herrmann, "Effect of the type of activated carbons on the photocatalytic degradation of aqueous organic pollutants by UV-irradiated titania," *Journal of Catalysis*, vol. 200, no. 1, pp. 10–20, 2001.

[13] M. Qamar, C. R. Yoon, H. J. Oh et al., "Effect of post treatments on the structure and thermal stability of titanate nanotubes," *Nanotechnology*, vol. 17, no. 24, pp. 5922–5929, 2006.

[14] M. Qamar, C. R. Yoon, H. J. Oh et al., "The effect of synthesis conditions on the formation of titanate nanotubes," *Journal of the Korean Physical Society*, vol. 49, no. 4, pp. 1493–1496, 2006.

[15] H. J. Oh, K. J. Noh, H. K. Ku et al., "Preparation of various metal ions doped hydrogen titanate nano particle coated thin films by layer-by-layer self-assembling method for an electrochromic electrode," *Progress in Organic Coatings*, vol. 74, no. 4, pp. 745–749, 2012.

[16] H. J. Oh, K. J. Noh, H. K. Ku et al., "Preparation of hydrogen titanate nanotube/FTO glass thin film obtained by the layer-by-layer-self assembling method for water splitting," *Journal of Nanoscience and Nanotechnology*, vol. 11, pp. 7210–7213, 2011.

[17] M. Qamar, C. R. Yoon, H. J. Oh et al., "Preparation and photocatalytic activity of nanotubes obtained from titanium dioxide," *Catalysis Today*, vol. 131, no. 1–4, pp. 3–14, 2008.

[18] W. B. Ingler Jr. and S. U. M. Khan, "Photoresponse of spray pyrolytically synthesized magnesium-doped iron (III) oxide (p-Fe_2O_3) thin films under solar simulated light illumination," *Thin Solid Films*, vol. 461, no. 2, pp. 301–308, 2004.

[19] Y. S. Hu, A. Kleiman-Shwarsctein, A. J. Forman, D. Hazen, J. N. Park, and E. W. McFarland, "Pt-doped α-Fe_2O_3 thin films active for photoelectrochemical water splitting," *Chemistry of Materials*, vol. 20, no. 12, pp. 3803–3805, 2008.

[20] Z. Xu and J. Yu, "Visible-light-induced photoelectrochemical behaviors of Fe-modified TiO_2 nanotube arrays," *Nanoscale*, vol. 3, no. 8, pp. 3138–3144, 2011.

[21] J. Zhang, J. Yu, Y. Zhang, Q. Li, and J. R. Gong, "Visible light photocatalytic H_2-production activity of CuS/ZnS porous nanosheets based on photoinduced interfacial charge transfer," *Nano Letters*, vol. 11, pp. 4774–4779, 2011.